

RSC Advances



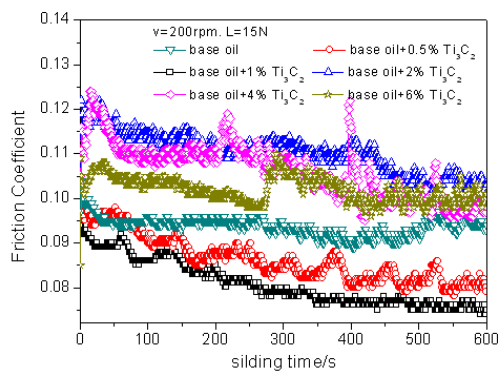
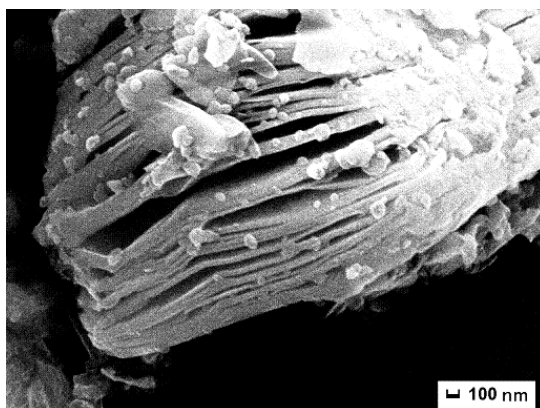
This is an *Accepted Manuscript*, which has been through the Royal Society of Chemistry peer review process and has been accepted for publication.

Accepted Manuscripts are published online shortly after acceptance, before technical editing, formatting and proof reading. Using this free service, authors can make their results available to the community, in citable form, before we publish the edited article. This *Accepted Manuscript* will be replaced by the edited, formatted and paginated article as soon as this is available.

You can find more information about *Accepted Manuscripts* in the [Information for Authors](#).

Please note that technical editing may introduce minor changes to the text and/or graphics, which may alter content. The journal's standard [Terms & Conditions](#) and the [Ethical guidelines](#) still apply. In no event shall the Royal Society of Chemistry be held responsible for any errors or omissions in this *Accepted Manuscript* or any consequences arising from the use of any information it contains.

Graphical abstract

two-dimensional $\text{Ti}_3\text{C}_2(\text{OH})_2$ nanosheets and tribological properties for oil-based additives

Cite this: DOI: 10.1039/c0xx00000x

www.rsc.org/xxxxxx

ARTICLE TYPE

Preparation and tribological properties of $\text{Ti}_3\text{C}_2(\text{OH})_2$ nanosheets as additive in base oil

Xianghua Zhang^{a,b}, Maoquan Xue^{*b,c}, Xinghua Yang^c, Zhiping Wang^c, Guangsi Luo^c, Zhide Huang^c, Xiaoli Sui^c and Changsheng Li^{*b}

Received (in XXX, XXX) Xth XXXXXXXXXX 20XX, Accepted Xth XXXXXXXXXX 20XX

DOI: 10.1039/b000000x

The two-dimensional $\text{Ti}_3\text{C}_2(\text{OH})_2$ nanosheets were synthesized by exfoliation of laminated Ti_3AlC_2 in HF and characterized by X-ray diffractometer, SEM, TEM, and HRTEM. The results indicated that the $\text{Ti}_3\text{C}_2(\text{OH})_2$ compounds had 2D layer-like structures with thickness of 10–20 nm, and the fabrication process of $\text{Ti}_3\text{C}_2(\text{OH})_2$ nanosheets was discussed on the basis of the experimental facts. The tribological properties of $\text{Ti}_3\text{C}_2(\text{OH})_2$ nanosheets as additives in base oil were investigated by UMT-2 ball-on-disc tribotester. Under the determinate conditions, the friction coefficient of the base oil containing $\text{Ti}_3\text{C}_2(\text{OH})_2$ nanosheets was lower than that of the base oil under 15 N load with 200 rpm, and decreased with increasing mass fraction of $\text{Ti}_3\text{C}_2(\text{OH})_2$ nanosheets when it was <1.0 wt.%. A combination of sliding friction, and stable tribofilm on the rubbing surface could explain the improved tribological properties of $\text{Ti}_3\text{C}_2(\text{OH})_2$ nanosheets as additives.

1. Introduction

In recent years, tremendous attention has been paid to two-dimensional (2D) nanosheets due to their exotic structural feature of two-dimensional anisotropy and physicochemical properties, which differ from those of their 3D (bulk) counterparts.^{1–11} Graphene, as a typical two-dimensional crystals with an inherent zero band gap, has been the most widely studied 2D material during the past few years owing to its exceptional electronic, thermal, mechanical, optical properties compared with bulk crystals graphite.^{12–20} Inspired by the graphene nanosheets, various two-dimensional (2D) materials (h-BN, transition metal dichalcogenides and transition metal oxides) have attracted great attention due to their unique properties compared to graphene. In recent studies, these compounds have a variety of important applications, such as in solid lubricants²¹, solar cells²², and nanocrystallites phototransistors²³, photodetectors,²⁴ electroluminescent devices²⁵ and electrocatalysis²⁶.

Very recently, a novel family of 2D-like transition metal nanocarbides and nanonitrides named MXenes, was prepared by exfoliating the counterpart MAX phases in hydrofluoric acid.^{27,28} MAX phases are a large family (>60 members) of ternary transition metal carbides and/or nitrides with a general formula of

$\text{M}_{n+1}\text{AX}_n$, where M is an early transition metal, A is an A group element (mostly IIIA or IVA group), X is C or N, $n=1, 2, 3, \dots$, it was found that MAX phases has excellent tribological property as lubrication additive.^{29–31} To date, the as synthesized MXene phases include Ti_2C , Ti_3C_2 , Ta_4C_3 , $(\text{Ti}_{0.5}\text{Nb}_{0.5})_2\text{C}$, $(\text{V}_{0.5}\text{Cr}_{0.5})_3\text{C}_2$, V_2C , Nb_2C and Ti_3CN . The present study found that MXenes have displayed interesting properties and have many potential applications³². For example, the conductivity of multilayered MXenes was found comparable to that of multilayered graphene.^{33–34} Naguib et al.³⁵ discovered that MXenes are promising as anode materials for Li-ion batteries. Sun et al.³⁶ found that Ti_3C_2 after intercalation with dimethyl sulfoxide had an obvious higher capacity than that before intercalation as anode for lithium ion batteries.

Theoretical studies regarding different properties also began soon after the experimental discovery of MXene systems. Khazaei et al.³⁷ using the Boltzmann theory and first-principles electronic structure calculations, have predicted the thermoelectric properties of more than 35 different functionalized MXene monolayers and their corresponding multilayers, and found that Mo_2C acquire superior thermoelectric properties among all MXenes. Shein and Ivanovskii employing first-principle band structure calculations, have studied the structural, electronic properties and relative stability of the MXene $\text{Ti}_{n+1}\text{C}_n$ and $\text{Ti}_{n+1}\text{N}_n$ ($n = 1, 2$ and 3). Density functional theory (DFT) calculations showed that MXenes can be semiconductors with tunable band gap that can be controlled by changing the surface termination, but nonterminated MXenes are metallic and are expected to have the highest conductivity. Kurtoglu et al. have estimated the in-plane elastic constants of MXenes, using DFT, to

^a School of Mechanical Engineering, Jiangsu University of Technology, Changzhou, Jiangsu Province, 213001, P.R. China

^b School of Materials Science and Engineering, Jiangsu University, Zhenjiang, Jiangsu Province, 212013, P.R.China; E-mail: changshengli2008@163.com

^c Changzhou Institute of Light Industry Technology, Changzhou, Jiangsu Province, 213164, P.R.China; E-mail: xuemaog@163.com

be more than 500 GPa, which means that MXenes are expected to have higher stiffness than structural steel (400 GPa).³⁸⁻⁴¹

The first MXene was fabricated by exfoliation Ti_3AlC_2 in hydrofluoric acid solutions, so Al atoms with relatively weak bond is selectively etched away.²⁷ However, there are few studies focus on the details of these new 2D materials fabrication process, therefore, it is still a great challenge to control the morphology and fascinating structure by adjusting the reaction conditions, also, to the best of our knowledge, its application as lubricating additive for base oil has rarely been investigated.

In this work, the graphene-like $\text{Ti}_3\text{C}_2(\text{OH})_2$ was successfully prepared by etching layered Ti_3AlC_2 . The evolution of morphology and internal structure with the increasing of reaction time was systematically investigated, the tribological properties of $\text{Ti}_3\text{C}_2(\text{OH})_2$ nanosheets as base oil additives were also investigated. This study enriches the understanding of the etching process of the MAX phases and will be useful for MXene practical application in the future.

2. Experimental

2.1 Synthesis of Exfoliated $\text{Ti}_3\text{C}_2(\text{OH})_2$

Pre-reacted, Ti_3AlC_2 powders were prepared by pressureless sintering in Ar atmosphere from powder mixture of Ti, Al, C and Sn, as described elsewhere²⁹. Briefly, this material was prepared according to the following procedure: mixed powders of Ti, Al, graphite and Sn with stoichiometric proportion of $3\text{Ti}/1\text{Al}/1.8\text{C}/0.2\text{Sn}$ were magnetic stirring in absolute alcohol at 70°C . After being dried and sieved, the powders were cold-pressed into a disc with 25mm diameter in a stainless steel die. Then, the cold pressing slices were sintered under an Ar atmosphere in tube furnace. The synthesis temperature was 1400°C . Finally, samples were crushed and grinded into powder.

The exfoliation process was carried as follows: Roughly, 3 g of Ti_3AlC_2 powders were immersed in 70 ml of a 40% concentrated HF solution, the mixture was then stirred with different times at room temperature. The resulting suspension was subsequently filtered and washed with ethanol several times. Finally, it was dried in vacuum at 70°C for 12 h, and the 2D $\text{Ti}_3\text{C}_2(\text{OH})_2$ was obtained.

2.2 Characterisation of $\text{Ti}_3\text{C}_2(\text{OH})_2$ samples

To investigate the phase and structural changes occurring as a result of the HF exfoliation, X-ray diffraction, XRD, patterns were collected using a diffractometer with Cu-K α radiation, operating at 40 kV and 20 mA, $\lambda=0.1546$ nm, respectively, data analysis with Jade software. The morphological changes occurring upon exfoliation were investigated using a scanning electron microscope (SEM, JEOL JXA-840A), and a transmission electron microscope, TEM, (JEOL JEM-100CX II, Japan) using an accelerating voltage of 200 kV. All the measurements were carried out at room temperature.

2.3 Tribological properties of 2D $\text{Ti}_3\text{C}_2(\text{OH})_2$ as lubrication additive

Different mass fractions of the as-prepared $\text{Ti}_3\text{C}_2(\text{OH})_2$ powders were dispersed in 100SN base oil via 2 h ultrasonication without

any active reagent, and then a series of suspended oil samples were obtained. The tribological properties of the oil containing $\text{Ti}_3\text{C}_2(\text{OH})_2$ were investigated using a universal tribotester (UMT-2, Center for Tribology Inc., USA). The friction and wear tests were performed at a rotating speeds of 200 rpm with loads of 5-50 N, for the test duration of 10 min. The material of the upper sample is 440C stainless steel ball with a diameter of 10 mm, hardness of 62 HRC, and the counterpart is 45# steel disc of $\Phi 30$ mm \times 3 mm in size. The friction coefficient was recorded automatically and the wear scars widths were measured by a conventional optical microscope. Morphologies of wear scars were examined using a JSM-5600LV scanning electron microscope (SEM). The elements of the friction surface were analyzed using energy-dispersive X-ray spectroscopy (EDS).

3. Results and Discussion

The XRD patterns of the samples exfoliated by HF with different times are illustrated in Fig.1. It can be seen that all characteristic peaks of Ti_3AlC_2 are almost the same and become stronger, and no peak of other phases appears when Ti_3AlC_2 exfoliated by HF for 10 hours, may be the HF solution react with a small amount of impurity depositing on the surface of Ti_3AlC_2 particles, which leads to products more purer⁴². If the treating time reaches to 60 hours, no peaks corresponding to Ti_3AlC_2 exists and TiC peaks at $35-42^\circ$ have little change, characteristic peaks corresponding to $\text{Ti}_3\text{C}_2(\text{OH})_2$ appeared, which is obeys to the calculated structure²⁵. When the treating time further increases to 80 hours, the characteristic peaks corresponding to $\text{Ti}_3\text{C}_2(\text{OH})_2$ have little change. As reaction time prolongs to 100 hours, the characteristic peaks corresponding to $\text{Ti}_3\text{C}_2(\text{OH})_2$ become weaker and broader, which indicates that the long time exfoliation may decrease structural order degree of products. Therefore, the relatively weak metallic bonding between Ti, Al was interrupted by etch off Al atom in the process of HF treatment, so as to make the hydroxyl groups attached on the surface of exposed Ti_3C_2 , forming $\text{Ti}_3\text{C}_2(\text{OH})_2$.

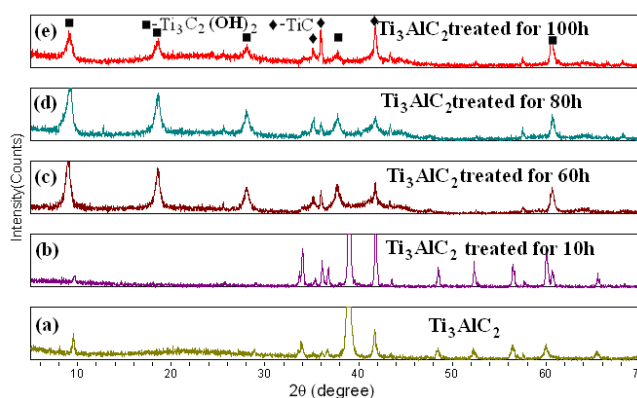


Fig. 1 XRD patterns of Ti_3AlC_2 powders after HF treatment for different time.

The morphology and microstructure of exfoliated products were examined by SEM, it was found that the exfoliated products were visibly influenced by the HF treated time. SEM observation in Fig.2a shows that after exfoliated by HF for 10 hours, the product still consists of a number of lamellar grains

with densely aligned layered structures, similar with the unexfoliated Ti_3AlC_2 ^{27,38}. When the exfoliating time increases to 60 hours, in comparison with the 10 hours (Fig. 2a), a small amount of slight delamination arises as shown in Fig. 2b. With the increase of the treating time, the more Al atoms dislodged from the structure makes the gradual separation of layers (Fig. 2c,d). the layers are clearly separated from each other after HF treatment for 100 hours (Fig. 2d), is analogous to results of exfoliated graphite^{43,44}. The thickness of the layered $\text{Ti}_3\text{C}_2(\text{OH})_2$ is about 10-20 nm. According to the above observations, it was concluded that 2D nanosheets were successful exfoliated by corrosion of layered Ti_3AlC_2 in hydrogen fluoride for a certain period of time.

The morphology and microstructure of the products prepared after HF treatment for 100 h were further investigated by TEM (shown in Fig.3). Fig.3a shows the TEM of the as-synthesized $\text{Ti}_3\text{C}_2(\text{OH})_2$ nanocrystals. It was found that after ultrasonic treatment the two-dimension nanosheets were obtained, the nanosheets is quite thin and shows individual layer or stack of several layers. In Fig.3b, the lattice fringe spacing between two adjacent crystal planes of the nanosheets was determined to be 0.2656 nm in the HRTEM image. The corresponding SAED pattern in Fig.3c shows the lattice plane is hexagonal symmetric.

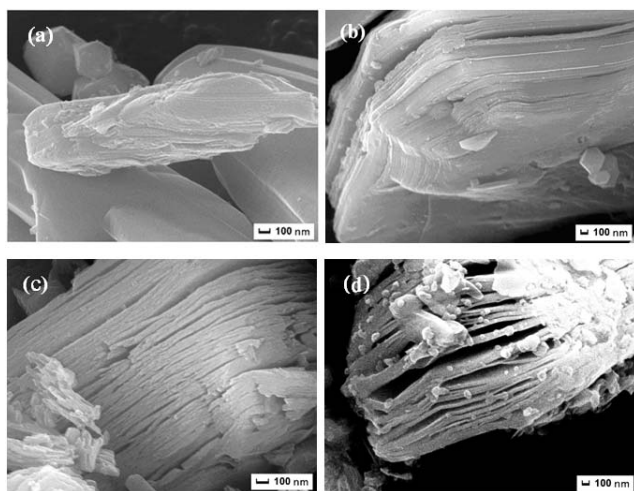


Fig.2 SEM images of Ti_3AlC_2 after HF treatment for (a)10h, (b)60h, (c)80h, and (d)100h.

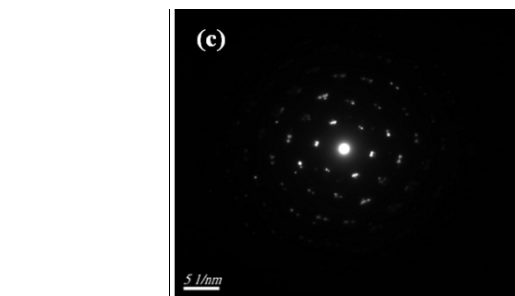
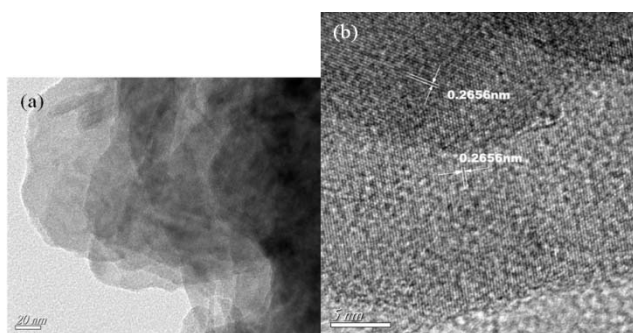
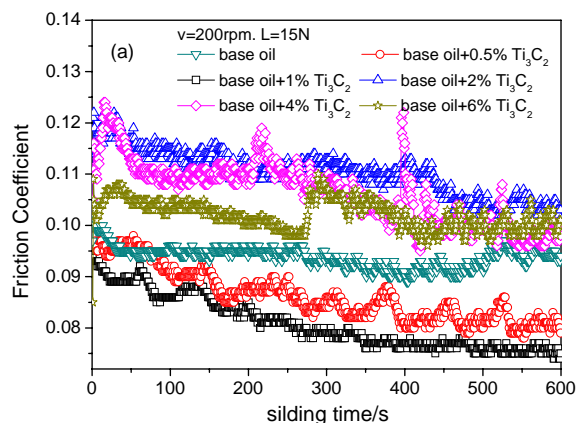


Fig.3 TEM images of Ti_3AlC_2 after HF treatment for 100h (a)TEM, (b)HRTEM, (c)SAED

The tribological behaviors of the as-prepared 2D $\text{Ti}_3\text{C}_2(\text{OH})_2$ nanosheets as lubrication additive in 100SN base oil under 15 N load with 200rpm were investigated by a UMT-2 ball-on-disc friction and wear tester. The effect of additives concentration on the friction coefficient and wear scar width is displayed in Fig.4. It is found that in Fig. 4a, with the concentration of 0-1 wt%, the friction coefficients decreases slightly and presents little fluctuation with the sliding distance, while the friction coefficients with other concentration (2-6 wt%) displays high value and acute fluctuation with the sliding distance. And the base oil presents best friction-reducing performance with 1.0 wt% concentration.

Fig. 4 b gives the wear scar width (WSW) vs. the different $\text{Ti}_3\text{C}_2(\text{OH})_2$ concentrations. It can be seen that the wear scar width of base oil is slight increases by adding $\text{Ti}_3\text{C}_2(\text{OH})_2$ nanosheets, the wear scar width of base oil containing 0-1.0 wt% $\text{Ti}_3\text{C}_2(\text{OH})_2$ nanosheets is a little smaller than that of oil containing 2-6 wt%, which is in good accordance with the unstable and increasing friction coefficient value in Fig. 4a. Therefore, the most appropriate additive amount of the 2D $\text{Ti}_3\text{C}_2(\text{OH})_2$ is 1.0 wt%. This can be attributed to the fact that the dispersivity of 2D $\text{Ti}_3\text{C}_2(\text{OH})_2$ is good for 1.0 wt% concentration, therefore, two mating wear surfaces were filled with the dispersed nanosheets during the wear process, and then $\text{Ti}_3\text{C}_2(\text{OH})_2$ nanosheets on wear surface could form a layer of tribofilm, preventing rough contact between the two mating wear surfaces. In addition, the two-dimensional sheet shape of $\text{Ti}_3\text{C}_2(\text{OH})_2$ nanosheets could provide very easy shear and more easily a slider between the two mating wear surfaces, so the friction coefficient of base oil with $\text{Ti}_3\text{C}_2(\text{OH})_2$ nanosheets decreases.



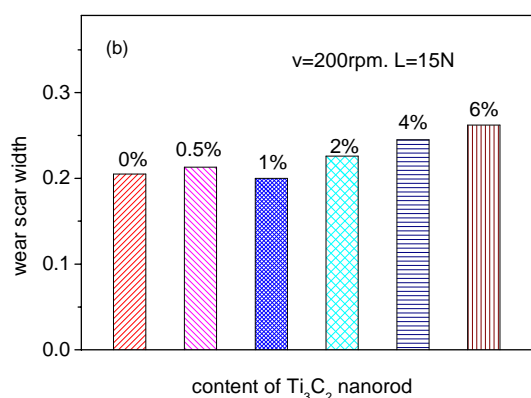


Fig. 4 (a) Friction coefficient as a function of sliding distance, (b) wear scar width on disc specimens lubricated with different concentrations $Ti_3C_2(OH)_2$ nanosheets in 100SN base oil.

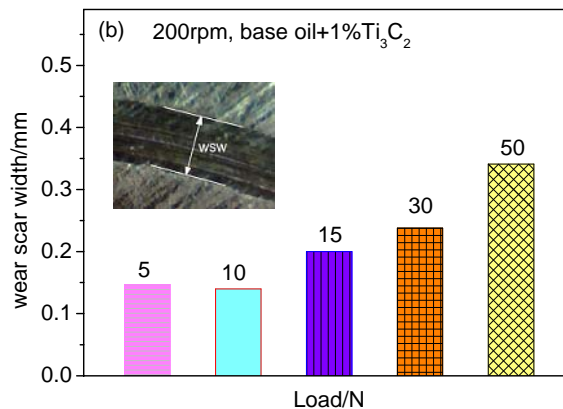
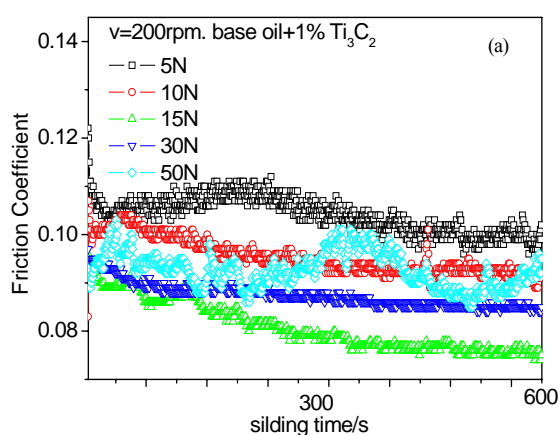


Fig. 5 (a) Friction coefficient, (b) wear scar width of base oil mixed with 1.0wt% $Ti_3C_2(OH)_2$ nanosheets additive under different loads at 200rpm for 10min..

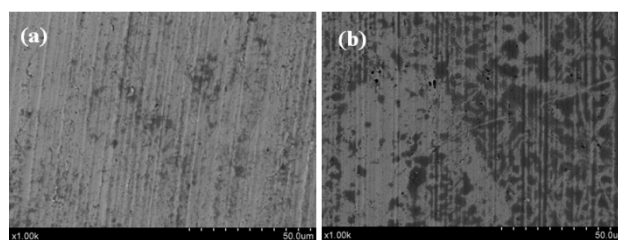
The effect of applied load on the friction coefficient and wear scar width of base oil containing 1.0 wt% 2D $Ti_3C_2(OH)_2$ nanosheets is presented in Fig.5. Fig. 5a shows the friction coefficients vs. sliding distance curves of base oil containing 1.0 wt% $Ti_3C_2(OH)_2$ nanosheets under different normal loads (5–50 N). It is found that under lower load (e.g. 5 N), the friction coefficient is unstable and vary in the range of 0.101–0.113. However, under the load of 10–30 N, the friction coefficient decreases slightly and becomes stable at about 0.075–0.092 with the sliding distance. The friction coefficient displays acute fluctuation and high value at high load of 50N, the base oil containing 1.0 wt% 2D $Ti_3C_2(OH)_2$ presents better friction-reducing performance under the load of 15N.

Fig. 5b shows the wear scar width (WSW) of 100SN base oil containing 1.0 wt% synthesized $Ti_3C_2(OH)_2$ at different loads. It can be observed that the WSW of the base oil with 1.0 wt% $Ti_3C_2(OH)_2$ additives increase gradually with an increase of the applied load. Consequently, the addition of $Ti_3C_2(OH)_2$ can efficiently improve the friction properties of 100SN base oil with 1.0 wt% $Ti_3C_2(OH)_2$. The lubrication of $Ti_3C_2(OH)_2$ as oil additive is mainly dependent on the formation of tribofilm in the friction process. However, a continuous tribofilm only begins to be formed under an optimal load. For the higher load, the tribofilm became unstable and easily damaged, result in a high wear scar width, and the friction coefficient became fluctuant, as shown in Fig. 5a.



The topography of the worn scar lubricated by base oil with various contents of $Ti_3C_2(OH)_2$ nanosheets under 15 N was investigated using SEM, as shown in Fig.6. This SEM image in Fig. 6a shows that the rubbed surface lubricated by the pure base oil is evidently rough with lots of wide and deep furrows because of contact fatigue. In Fig. 6b,c, the worn surface lubricated with base oil added 0.5 and 1.0 wt% $Ti_3C_2(OH)_2$ nanosheets smoother than that lubricated with pure base oil. The furrows are shallower and no obvious mechanical damage on the worn surface of steel disc lubricated by base oil with 0.5 and 1.0 wt% $Ti_3C_2(OH)_2$, at the same time, a thin tribofilm is formed on the substrate. However, the concentration of $Ti_3C_2(OH)_2$ higher to 6.0 wt%, as presented in Fig. 6d, the worn surface becomes evidently rough and the plastic deformation is severe, which is in good accordance with the friction coefficient of base oil with 6.0 wt% $Ti_3C_2(OH)_2$ nanosheets is unstable and higher than that with 0.5 and 1.0 wt% $Ti_3C_2(OH)_2$, as shown in Fig.4a.

Thus, the mechanism of the reducing friction and antiwear of nanosheets dispersed in base oil can be confirmed by the results of SEM. In this work, it has been shown that the base oil with a certain viscosity containing 1.0 wt% $Ti_3C_2(OH)_2$ nanosheets can form a uniform tribofilm, which can decrease shearing stress, therefore, give a low friction coefficient and wear scar width. In the friction process, because of the contact pressure creating traction-compression stressed zones, a thin tribofilm is formed on the metal substrate, the tribofilm could not only withstand the load of the steel ball but also prevent from direct contact of two mating pairs. Therefore, the antiwear ability of the base oil with 1.0 wt% $Ti_3C_2(OH)_2$ nanosheets was improved, and the friction coefficient was decreased significantly and remained constant. However, too much higher concentration of the $Ti_3C_2(OH)_2$ nanosheets could destroy the stability of the colloid system of the base oil^{30,45-46}.



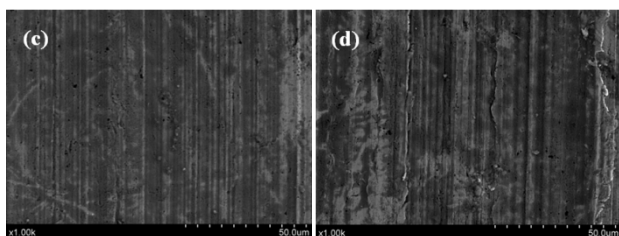


Fig.6 SEM images of the worn surfaces under 15N at 200rpm lubricated by pure base oil(a),and base oil with 0.5wt%(b), 1.0wt%(c), and 6.0 wt%(d) $\text{Ti}_3\text{C}_2(\text{OH})_2$ nanosheets

In order to confirm the formation of the tribofilm and its composition, the corresponding EDS analysis of the worn surface of the steel disc lubricated by base oil with 1.0 wt% $\text{Ti}_3\text{C}_2(\text{OH})_2$ nanosheets was carried out. As shown in Fig. 7, peaks from titanium and carbon atoms indicated the formation of a tribofilm. It is believed that the smooth and flat surface lubricated by composites results from the deposition of $\text{Ti}_3\text{C}_2(\text{OH})_2$ tribofilm on the friction surface.

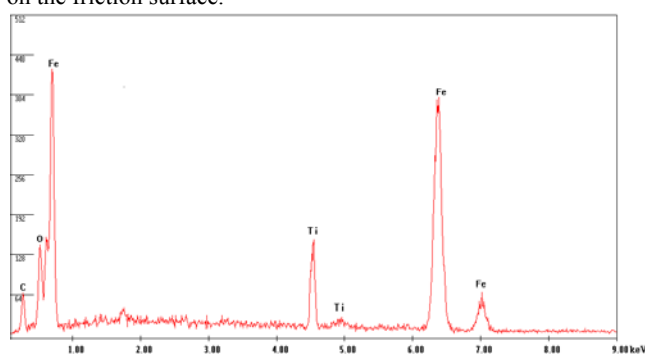


Fig.7 EDS spectrum of the worn surface of the steel disc lubricated by base oil with 1.0 wt% $\text{Ti}_3\text{C}_2(\text{OH})_2$ nanosheets

4. Conclusion

In summary, $\text{Ti}_3\text{C}_2(\text{OH})_2$ nanosheets with thickness of 10-20 nm were successfully exfoliated via corrosion reaction by immersing Ti_3AlC_2 powders in hydrofluoric acid for a certain period of time. As-prepared $\text{Ti}_3\text{C}_2(\text{OH})_2$ nanosheets as a lubricant additive can effectively improve the friction-reducing and anti-wear ability under the optimum concentration (1.0 wt.%). Tribological experiments indicated that the effect of $\text{Ti}_3\text{C}_2(\text{OH})_2$ nanosheets as lubrication additive could be attributed to the sliding friction of the $\text{Ti}_3\text{C}_2(\text{OH})_2$ nanosheets between the rubbing surfaces. Meanwhile, a stable tribofilm on the rubbing surface could not only bear the load of the steel ball but also prevent direct contact between the two rubbing surfaces.

Acknowledgements

This work was supported by the National Natural Science Foundation of China (51275213, 51302112), the Natural Science Foundation of the Jiangsu Higher Education Institutions of China (14KJB460012), and Scientific and Technological Innovation Plan of Jiangsu Province (CXLX12_0636).

Notes and references

- J. N.Coleman, M.Loty and A.O'Neill, *Science*, 2011, **331**,568.
- J.Feng, X.Sun and C.Wu, *Journal of the American Chemical Society*, 2011, **133**,17832.
- M.Chhowalla, H. S.Shin and G.Eda, *Nature chemistry*, 2013, **5**,263.
- M.Osada and T.Sasaki, *Advanced Materials*, 2012, **24**, 210.
- X.Zhou, J.Jiang and T.Ding, *Nanoscale*, 2014, **6**, 11046.
- C.Fan, Z.Wei and S.Yang, *RSC Adv.*, 2014, **4**,775.
- V.Nicolosi, M.Chhowalla and M. G.Kanatzidis, *Science*, 2013, **340**,6139.
- O.Mashtalir, M.Naguib and V. N.Mochalin,*Nature comm.* 2013, **4**,1716.
- M.Chhowalla, H. S.Shin and G.Eda, *Nature chemistry*, 2013, **5**,263.
- I.Paszli and K.Laszlo, *Colloid and Polymer Science*, 2007, **285**,1505.
- I.Paszli I. and I.Mohammed-Ziegler, Z.Horvolgyi, *Colloid and Polymer Science*, 2007, **285**,1009.
- A. K.Geim and K. S. Novoselov, *Nature materials*, 2007, **6**,183.
- A. H. C.Neto, F.Guinea and N. M. R.Peres, *Reviews of modern physics*, 2009, **81**,109.
- P.Avouris, *Nano letters*, 2010, **10**, 4285.
- A. A.Balandin, *Nature materials*, 2011, **10**,569.
- X.Tian, S.Sarkar and A.Pekker, *Carbon*, 2014, **72**, 82.
- Y.Zhu, S.Murali and W.Cai, *Advanced materials*, 2010, **22**, 3906.
- D.Yoon, Y. W.Son and H.Cheong, *Nano letters*, 2011, **11**, 3227.
- M. A.Rafiee, J. Rafiee and Z.Wang, *ACS nano*, 2009, **3**,3884.
- F. J.Nelson, V.K.Kamineni and T.Zhang, *Applied Physics Letters*, 2010, **97**, 253110.
- C.Lee, Q.Li and W.Kalb, *Science*, 2010, **328**, 76.
- J.Qiu, M.Guo and X.Wang, *ACS applied materials & interfaces*, 2011, **3**,2358.
- Z.Yin, H.Li and H.Li, *ACS nano*, 2011, **6**,74.
- P.A.Hu, Z.Wen and L.Wang, *ACS nano*, 2012, **6**, 5988.
- R. S.Sundaram, M.Engel and A. Lombardo, *Nano letters*, 2013, **13**, 1416.
- X.Chen, B.Su and G.Wu, *Journal of Materials Chemistry*, 2012, **22**(11),1284.
- M.Naguib, M.Kurtoglu and V.Presser, *Advanced Materials*, 2011, **23**, 4248.
- M.Naguib, O.Mashtalir and J.Carle, *ACS nano*, 2012, **6**,1322.
- M.Xue, H.Tang and C. S. Li, *Advances in Applied Ceramics*, 2014, **113**,245.
- M.Xue, X.Zhang and H.Tang, *RSC Adv.*, 2014, **4**, 39280.
- X. Ji, Z.Yi, D.Zhang, *Ceramics International*, 2014, **40**, 6219.
- Y.Gao, L.Wang and Z. Li, *Solid State Sciences*, 2014, **35**: 62.
- Q.K. Hu, D.D. Sun and Q.H. Wu, *J. Phys. Chem. A* 2013, **117**, 14253.
- M.Naguib, V. N.Mochalin and M. W.Barsoum, *Advanced Materials*, 2014, **26**,992.
- M.Naguib, J.Come and B.Dyatkin, *Electrochemistry Comm.*, 2012, **16**, 61.
- D.D.Sun,M.S.Wang and Z.Y.Li, *Electrochemistry Comm.*, 2014,**47**, 80.
- M.Khazaei, M.Arai and T.Sasaki, *Physical Chemistry Chemical Physics*, 2014, **16**,7841.
- D.Er, J.Li and M.Naguib, *ACS applied materials & interfaces*, 2014, **6**,11173.
- M.Naguib, O.Mashtalir and M. R.Lukatskaya, *Chem. Comm.*, 2014.
- M.Ghidiu, M.Naguib and C.Shi, *Chem. Comm.*, 2014, **50**,9517.
- A.N.Enyashin and A.L.Ivanovskii, *Journal of Solid State Chemistry*, 2013, **207**,42.
- F.Chang, C.Li and J.Yang, *Materials Letters*, 2013, **109**, 295.
- W.Lv, D. M.Tang and Y. B.He, *Acs Nano*, 2009, **3**, 3730.
- V.G.Makotchenko, E. D.Grayfer and A. S. Nazarov, *Carbon*, 2011, **49**,3233.
- J. Yang, B. B.Chen and H.J.Song, *Crystal Research and Technology*, 2014.
- G.Bai, J.Wang and Z.Yang, *RSC Adv.*, 2014, **4**, 47096.